



**QUEEN'S  
UNIVERSITY  
BELFAST**

## **Water-in-CO<sub>2</sub> microemulsions stabilized by an efficient cationic surfactant**

Sagisaka, M., Saito, Tatsuya, T., Masashi, A., Yoshizawa, A., Blesic, M., Rogers, S., Shirin, A., Guittard, F., Hill, C., & Eastoe, J. (2020). Water-in-CO<sub>2</sub> microemulsions stabilized by an efficient cationic surfactant. *Langmuir*. <https://doi.org/10.1021/acs.langmuir.0c00970>

**Published in:**  
Langmuir

**Document Version:**  
Peer reviewed version

**Queen's University Belfast - Research Portal:**  
[Link to publication record in Queen's University Belfast Research Portal](#)

### **Publisher rights**

Copyright 2020 American Chemical Society. This work is made available online in accordance with the publisher's policies. Please refer to any applicable terms of use of the publisher.

### **General rights**

Copyright for the publications made accessible via the Queen's University Belfast Research Portal is retained by the author(s) and / or other copyright owners and it is a condition of accessing these publications that users recognise and abide by the legal requirements associated with these rights.

### **Take down policy**

The Research Portal is Queen's institutional repository that provides access to Queen's research output. Every effort has been made to ensure that content in the Research Portal does not infringe any person's rights, or applicable UK laws. If you discover content in the Research Portal that you believe breaches copyright or violates any law, please contact [openaccess@qub.ac.uk](mailto:openaccess@qub.ac.uk).

This document is confidential and is proprietary to the American Chemical Society and its authors. Do not copy or disclose without written permission. If you have received this item in error, notify the sender and delete all copies.

**Water-in-CO<sub>2</sub> microemulsions stabilized by an efficient catanionic surfactant**

Journal:	<i>Langmuir</i>
Manuscript ID	la-2020-00970b.R3
Manuscript Type:	Article
Date Submitted by the Author:	12-Jun-2020
Complete List of Authors:	Sagisaka, Masanobu; Hirosaki University , Graduate School of Science and Technology Saito, Tatsuya; Hirosaki University , Graduate School of Science and Technology Abe, Masashi; Hirosaki University , Graduate School of Science and Technology Yoshizawa, Atsushi; Hirosaki University , Department of Frontier Materials Chemistry Blesic, Marijana; Queen's University Belfast, School of Chemistry and Chemical Engineering Rogers, Sarah; ISIS-STFC Neutron Scattering Facility, Harwell Science and Innovation Campus Alexander, Shirin; Swansea University, College of Engineering Guittard, Frédéric; Universite Cote d'Azur Hill, Christopher; University of Bristol, School of Chemistry Eastoe, Julian; University of Bristol, School of Chemistry

SCHOLARONE™  
Manuscripts

1  
2  
3  
4  
5  
6  
7  
8  
9  
10  
11  
12  
13  
14  
15  
16  
17  
18  
19  
20  
21  
22  
23  
24  
25  
26  
27  
28  
29  
30  
31  
32  
33  
34  
35  
36  
37  
38  
39  
40  
41  
42  
43  
44  
45  
46  
47  
48  
49  
50  
51  
52  
53  
54  
55  
56  
57  
58  
59  
60

# Water-in-CO<sub>2</sub> microemulsions stabilized by an efficient catanionic surfactant

*Masanobu Sagisaka<sup>1\*</sup>, Tatsuya Saito<sup>1</sup>, Masashi Abe<sup>1</sup>, Atsushi Yoshizawa<sup>1</sup>, Marijana Blesic<sup>2</sup>,*

*Sarah E. Rogers<sup>3</sup>, Shirin Alexander<sup>4</sup>, Frédéric Guittard<sup>5</sup>, Christopher Hill<sup>6</sup>, Julian Eastoe<sup>6</sup>*

<sup>1</sup> Department of Frontier Materials Chemistry, Graduate School of Science and Technology, Hirosaki  
University, 3 Bunkyo-cho, Hirosaki, Aomori 036-8561, JAPAN

<sup>2</sup> School of Chemistry and Chemical Engineering, Queen's University Belfast, University Road, Belfast,  
BT7 1NN, U.K.

<sup>3</sup> ISIS-CCLRC, Rutherford Appleton Laboratory, Chilton, Oxon OX11 0QX, U.K.

<sup>4</sup> Energy Safety Research Institute (ESRI), Swansea University, Bay Campus, Swansea SA1 8EN, UK.

<sup>5</sup> Univ. Cote d'Azur, NICE-Lab, 61-63 av. S. Viel, 06200 Nice, France

<sup>6</sup> School of Chemistry, University of Bristol, Cantock's Close, Bristol BS8 1TS, U.K.

\*To whom all correspondence should be addressed

Masanobu SAGISAKA E-mail: [sagisaka@hirosaki-u.ac.jp](mailto:sagisaka@hirosaki-u.ac.jp) Phone and Fax: +81-172-39-3579

**Abstract**

1  
2  
3  
4 To facilitate potential applications of water-in-supercritical CO<sub>2</sub> microemulsions (W/CO<sub>2</sub> μEs)  
5  
6 efficient and environmentally responsible surfactants are required with low levels fluorination. As well  
7  
8 as being able to stabilize water-CO<sub>2</sub> interfaces, these surfactants must also be economical, prevent bio-  
9  
10 accumulation and strong adhesion, deactivation of enzymes, and also be tolerant to high salt environments.  
11  
12 Recently, an ion paired catanionic surfactant with environmentally-acceptable fluorinated C<sub>6</sub>-tails was  
13  
14 found to be very effective at stabilizing W/CO<sub>2</sub> μEs with high water-to-surfactant molar ratios ( $W_0$ ) up to  
15  
16 ~50 (Sagisaka, M. et al. *Langmuir*, **2019**, 35, 3445–3454). As the cationic and anionic constituent  
17  
18 surfactants alone did not stabilize W/CO<sub>2</sub> μEs, this was the first demonstration of surfactant synergistic  
19  
20 effects in W/CO<sub>2</sub> microemulsions. The aim of this new study is to understand the origin of these intriguing  
21  
22 effects by detailed investigations of nanostructure in W/CO<sub>2</sub> microemulsions using high pressure small-  
23  
24 angle neutron scattering (HP-SANS). These HP-SANS experiments have been used to determine the  
25  
26 headgroup interfacial area and volume, aggregation number and effective packing parameter (EPP). These  
27  
28 SANS data suggest the effectiveness of this surfactant originates from increased EPP and decreased  
29  
30 hydrophilic/CO<sub>2</sub>-philic balance, related to a reduced effective headgroup ionicity. This surfactant bears  
31  
32 separate C<sub>6</sub>F<sub>13</sub>-tails and oppositely-charged headgroups, and was found to have a EPP value similar to  
33  
34 that of a double C<sub>4</sub>F<sub>9</sub>-tail anionic surfactant (4FG(EO)<sub>2</sub>), which was previously reported to be one of most  
35  
36 efficient stabilizers for W/CO<sub>2</sub> μEs (maximum  $W_0$  = 60-80). Catanionic surfactants based on this new  
37  
38 design will be key for generating super-efficient W/CO<sub>2</sub> μEs with high stability and water solubilization.  
39  
40  
41  
42  
43  
44  
45  
46  
47  
48

49 **Keywords:** Supercritical CO<sub>2</sub>, Microemulsion, Catanionic Surfactant, Solubilizing Power, Small-Angle  
50  
51 Neutron Scattering  
52  
53  
54  
55  
56  
57  
58  
59  
60

## Introduction

Supercritical CO<sub>2</sub> (scCO<sub>2</sub>) is now widely used industrially as an alternative solvent to replace volatile organic compounds (VOCs) for organic synthesis, dry cleaning, polymerization, extraction, and nanomaterial processing amongst others<sup>1</sup>. For these applications there are numerous advantages of scCO<sub>2</sub> such as low cost, non-toxicity, non-flammability, natural abundance, a solvent quality tunable by control over pressure and temperature, and elimination of energy-consuming solvent evaporation steps in separation processes<sup>1</sup>. One of the drawbacks of pure scCO<sub>2</sub> for applications is the inherent low solubility of polar solutes: approaches to overcome this are required to help develop further industrial applications of scCO<sub>2</sub>. An obvious way to enhance low solubility is through formation of water-in-scCO<sub>2</sub> (W/CO<sub>2</sub>) dispersions, including microemulsions ( $\mu$ Es) and macroemulsions (emulsions): numerous surfactants have been tested to accomplish this task<sup>2-13</sup>. However, conventional hydrocarbon (HC) surfactants typically used for analogous water-oil  $\mu$ Es, including Aerosol-OT (sodium bis-(2-ethyl-1-hexyl) sulfosuccinate, AOT)<sup>14</sup>, are essentially incompatible with pure scCO<sub>2</sub><sup>3-7</sup>. On the other hand, some specialized tailor-made fluorocarbon (FC) surfactants have been found to display high affinity for scCO<sub>2</sub>, and are able to stabilize W/CO<sub>2</sub>  $\mu$ Es with modest water-to-surfactant molar ratios  $> 10$  ( $W_0 = [\text{water}]/[\text{surf}]$ ).<sup>7-13</sup> These CO<sub>2</sub>-philic FC surfactants may consist of either perfluoropolyether (PFPE)-tails, double FC-tail and FC-HC hybrid-tail structures.<sup>7-13</sup> For example, a single PFPE-tail surfactant (PFPECOONH<sub>4</sub>), a hybrid surfactant having perfluorohexyl and *n*-butyl tails (FC6-HC4), and double perfluorocarbon-tail surfactants (8FS(EO)<sub>2</sub>, 8FG(EO)<sub>2</sub> and 4FG(EO)<sub>2</sub>) (**Figure S1** for chemical structures) have been shown to stabilize W/CO<sub>2</sub>  $\mu$ Es with maximum  $W_0$  ( $W_0^{\text{max}}$ ) values up to 20, 80 and 45-80, respectively.<sup>7-13</sup> These surfactants mentioned are mainly anionic which presents problems for applications, including, difficulties of removing ionic surfactants from processes producing nanoparticles, deactivation with enzymatic reactions, surfactant-dye complexation in dyeing, and salting-out at high salinities typical in enhanced oil recovery (EOR)<sup>15-19</sup>. For industrial applications CO<sub>2</sub>-philic surfactants should ideally be composed of (1) CO<sub>2</sub>-philic tails with low fluorination for reducing cost and environmental impact, and (2) possess nonionic or weakly ionic headgroups to minimize salting out.

1 Earlier studies <sup>20,21</sup> investigated synergistic effects on interfacial properties of scCO<sub>2</sub>-philic  
2 surfactants by mixing HC, FC and FC-HC surfactants (**Figure S1**). Mixing commercial nonionic HC  
3 surfactants (TMN-6 and L31, **Figure S1**) with fluorinated surfactants reduced the critical microemulsion  
4 concentration (*c<sub>μc</sub>*), which is defined as the lowest surfactant concentration to yield a microemulsion,  
5 compared to the individual surfactants, however, synergistic effects were not observed in terms of the  
6 water-solubilization *W*<sub>0</sub> <sup>20</sup>. On the other hand, mixing 8FS(EO)<sub>2</sub> and FC6-HC4 (**Figure S1**) increased  
7 *W*<sub>0</sub><sup>max</sup> by only 3 compared with the value for each surfactant at 75 °C and 400 bar, showing a very small  
8 synergistic effect <sup>21</sup>.  
9  
10  
11  
12  
13  
14  
15  
16  
17

18 In earlier studies of surfactant mixtures in conventional solvents, the combination of anionic and  
19 cationic surfactants was shown to result in strong synergism in terms of interfacial properties, stability of  
20 vesicles, reverse-type molecular assemblies and W/O dispersions <sup>22,23</sup>. In these cases, synergism is  
21 understood to originate from electrostatic interactions between oppositely charged headgroups. These  
22 cationic:anionic surfactant mixtures have been simplified further still, by synthesizing pure catanionic  
23 surfactants excluding the counterions.<sup>24</sup>  
24  
25  
26  
27  
28  
29  
30  
31

32 A previous study reported synthesis of three pure catanionic surfactants ([C<sub>6</sub>F<sub>13</sub>mim][CF<sub>3</sub>]<sub>3</sub>S],  
33 [C<sub>6</sub>F<sub>13</sub>mim][C<sub>6</sub>F<sub>13</sub>S] and [C<sub>5</sub>F<sub>11</sub>mim][C<sub>5</sub>F<sub>11</sub>S], **Figure 1**) bearing environmentally-acceptable short chain  
34 FC tails, and studied formation and properties of W/CO<sub>2</sub> μEs.<sup>25</sup> One of the these surfactants, namely  
35 [C<sub>6</sub>F<sub>13</sub>mim][C<sub>6</sub>F<sub>13</sub>S], showed exceptional water-solubilizing power (*W*<sub>0</sub><sup>max</sup> = ~50), representing the first  
36 observation of surfactant synergism in W/CO<sub>2</sub> μEs. The catanionic surfactants were shown to display  
37 cloud point temperatures, rather than Kraft temperatures, suggesting the catanionic headgroup has some  
38 nonionic character<sup>25</sup>.  
39  
40  
41  
42  
43  
44  
45  
46  
47

48 To clarify the mechanism of synergism and ion pairing with these CO<sub>2</sub>-active catanionic  
49 surfactants this study investigates phase behavior, solubilizing properties and self-assembly structure of  
50 W/CO<sub>2</sub> μEs at different pressures and *W*<sub>0</sub> values. Probe dye studies, using UV-vis absorption spectra with  
51 an ionic dye methyl orange was used to follow water uptake and high-pressure small-angle neutron  
52 scattering (HP-SANS) was used to determine microemulsion water droplet structures and sizes. The  
53  
54  
55  
56  
57  
58  
59  
60

SANS measurements have permitted an assessment of the effective packing parameter (EPP, in other words, an intrinsic packing parameter relevant to an individual mixed system under certain experimental conditions)<sup>26-29</sup> to be made. The EPP is a key index, indicating the preferred self-assembly structure, and is based on surfactant spatial packing, resulting from interactions with solvents (water and CO<sub>2</sub>) and neighboring surfactant molecules. These results demonstrate that cationic surfactants can offer new insight into the design criteria for inexpensive and environmental-friendly surfactants for W/CO<sub>2</sub> μEs appropriate for industrial use.

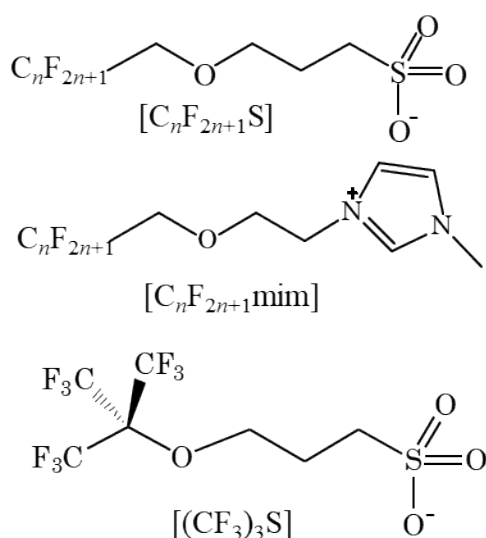


**Figure 1** Chemical structures of surfactant ions ( $n = 5$  or  $6$ ).

## Experimental Section

### Materials

The catanionic surfactants  $[\text{C}_6\text{F}_{13}\text{mim}][(\text{CF}_3)_3\text{S}]$ ,  $[\text{C}_6\text{F}_{13}\text{mim}][\text{C}_6\text{F}_{13}\text{S}]$  and  $[\text{C}_5\text{F}_{11}\text{mim}][\text{C}_5\text{F}_{11}\text{S}]$  (**Figure 1**, purity > 95 %) used here were synthesized and purified as described in a previous study<sup>25</sup>. Ultrapure water with a resistivity of 18.2 M $\Omega$  cm was obtained from a Millipore Milli-Q Plus system. CO<sub>2</sub> was of 99.99% purity (Ekika Carbon Dioxide Co., Ltd.). Methyl orange was purchased from Acros organics and used without further purification.

### Phase behavior observations and UV-visible absorption spectroscopy

A high-pressure (HP) cell with a metal-to-glass sealed glass window (KP-308-3, Nihon Klingage co., ltd) and a moveable piston inside the cell was employed to examine the phase behaviour of surfactant/water/scCO<sub>2</sub> mixtures by operating pressure and temperature. A detailed description of the experimental apparatus and procedures is given in earlier papers.<sup>12,13,25</sup>

Uptake of water into W/CO<sub>2</sub>  $\mu\text{Es}$  was examined by UV-visible absorption spectroscopy measurements in a pressure cell (stainless steel SUS316: cell volume 1.5 cm<sup>3</sup>) with three quartz windows (thickness: 8 mm, inner diameter: 10 mm). The spectral measurements were performed with a double-beam spectrophotometer (Hitachi High-Technologies, Co., U-2810). Each window was positioned to provide a perpendicular 10-mm optical path. The windows were attached and fastened tightly to the stainless steel body of the cell with PTFE kel-F packing, thereby compressing the packing between the stainless steel parts and the windows, providing excellent sealing (tested up to 400 bar); temperature was controlled by circulating water thermostat bath.

The spectroscopic measurements of the water/surfactant/scCO<sub>2</sub> systems were performed at 350 bar and 45 or 75 °C. The densities of CO<sub>2</sub> were calculated using the Span-Wagner equation of state (EOS)<sup>30</sup>. Pre-determined amounts of surfactant and CO<sub>2</sub>, where the molar ratio of surfactant to CO<sub>2</sub> was fixed at  $8 \times 10^{-4}$ , were loaded into the optical cell. An aqueous solution containing methyl orange (MO) as a



1 trace marker dye (3 mM) was then added into the optical cell through a six-port valve until the clear  
2 single-phase Winsor-IV W/CO<sub>2</sub> μE microemulsion converted into a turbid emulsion or hydrated  
3 surfactant was seen to precipitate. During spectroscopic measurements, the scCO<sub>2</sub> mixtures were stirred  
4 by a magnetic stirrer.  
5  
6  
7  
8  
9

## 12 High-Pressure small-angle neutron scattering (SANS) measurements and data analyses

15 Due to the range of neutron wavelengths available, time-of-flight (T-O-F) SANS is suitable for  
16 studying the shapes and sizes of colloidal systems. High-pressure SANS (HP-SANS) is a particularly  
17 important technique for determining aggregated nanostructures in supercritical CO<sub>2</sub><sup>10,12,13,25</sup>. The HP-  
18 SANS measurements were performed at 45 °C at various pressures using the SANS2D T-O-F instrument,  
19 at the Rutherford Appleton Laboratory at ISIS UK, in conjunction with a stirred, high-pressure cell (Thar).  
20 The cell path length and the incident neutron beam diameter were both 10 mm. The measurements gave  
21 absolute scattering cross sections  $I(Q)$  (cm<sup>-1</sup>) as a function of momentum transfer  $Q$  (Å<sup>-1</sup>), which is defined  
22 as  $Q = (4\pi/\lambda)\sin(\theta/2)$ , where  $\theta$  is the scattering angle. The accessible  $Q$  range was 0.002-1.0 Å<sup>-1</sup> on  
23 SANS2D arising from a white neutron beam with incident wavelengths,  $\lambda$ , of 2.2-10 Å. The data were  
24 normalized for transmission, empty cell, solvent background, and pressure induced changes in cell volume  
25 as before<sup>12,13,25</sup>.  
26  
27  
28  
29  
30  
31  
32  
33  
34  
35  
36  
37  
38  
39

40 Pre-determined amounts of D<sub>2</sub>O and surfactant, where the molar ratio of surfactant to CO<sub>2</sub> was  
41 fixed at  $8.0 \times 10^{-4}$  (= 16.7 mM at the appropriate experimental condition), were loaded into the Thar cell.  
42 Then CO<sub>2</sub> (11.3 g) was introduced into the cell by using a high-pressure pump, and the  
43 surfactant/D<sub>2</sub>O/CO<sub>2</sub> mixture was pressurized to 120, 200 or 350 bar at 45 °C by decreasing the inner  
44 volume of the cell. Under vigorous stirring, visual observations were carried out to identify the mixture  
45 as being a transparent single-phase (W/CO<sub>2</sub> μE) or a turbid phase. Finally, the HP-SANS experiments  
46 were performed for not only single-phase W/CO<sub>2</sub>μEs, but also turbid phases formed below the cloud point  
47 phase transition pressure  $P_{\text{trans}}$ . Due to the systems being dilute dispersions (volume fractions typically ≤  
48  
49  
50  
51  
52  
53  
54  
55  
56  
57  
58  
59  
60

0.012), the physical properties of the continuous phase of scCO<sub>2</sub> were assumed to be equivalent to those of pure CO<sub>2</sub>. The scattering length density (SLD) of reversed micelle shells ( $\rho_{\text{shell}}$ ) was calculated as  $\rho_{\text{shell}} = 2.28 \times 10^{10} \text{ cm}^{-2}$ . The SLDs of CO<sub>2</sub> ( $\rho_{\text{CO}_2}$ ) and aqueous cores ( $\rho_{\text{core}}$ ) containing the catanionic headgroup in the D<sub>2</sub>O/CO<sub>2</sub>  $\mu\text{E}$  are variables of CO<sub>2</sub> density and  $W_0$ , and are estimated as;  $\rho_{\text{CO}_2} / (10^{10} \text{ cm}^{-2}) = 2.29$  at 350 bar, 2.03 at 200 bar, and 1.64 at 120 bar, and  $\rho_{\text{core}} / (10^{10} \text{ cm}^{-2}) = 3.34$  at  $W_0 = 5$ , 4.15 at  $W_0 = 10$ , 4.62 at  $W_0 = 15$ , 4.92 at  $W_0 = 20$ , 5.13 at  $W_0 = 25$ , 5.28 at  $W_0 = 30$  and 5.40 at  $W_0 = 35$  as estimated in supporting information (see **S2**). As  $\rho_{\text{shell}}$  was close to  $\rho_{\text{CO}_2}$  and the shells are solvated with CO<sub>2</sub>, neutron scattering from the shells was assumed to be negligible owing to the small contrast step. Therefore, SANS from the D<sub>2</sub>O/CO<sub>2</sub>  $\mu\text{E}$ s was assumed to only be from the so-called aqueous core contrast. For model fitting data analysis, the W/CO<sub>2</sub>  $\mu\text{E}$  droplets were treated as ellipsoidal particles with a Schultz distribution in core radii<sup>31</sup>. The polydispersities in ellipsoid radii were fixed at 0.3 as found in spherical D<sub>2</sub>O/CO<sub>2</sub>  $\mu\text{E}$ s with the double FC-tail surfactants (polydispersity = 0.17-0.40)<sup>12,13,25</sup>. Full accounts of the scattering laws are given elsewhere<sup>12,13,25,32</sup>. Data have been fitted to the models described above using the SasView small-angle scattering analysis software package (<http://www.sasview.org/>)<sup>12,13,25,32</sup>. The fitted parameters are the core radii perpendicular to the rotation axis ( $R_{\text{f-ell,a}}$ ) and along the rotation axis ( $R_{\text{f-ell,b}}$ ) for ellipsoidal particles; prior to full model fitting micellar dimensions were initially estimated by Guinier analysis ( $R_{\text{g-sph}}$ )<sup>33</sup>. The catanionic reverse micelles have C<sub>6</sub>-perfluorocarbon tails shells, which weakly interact with other<sup>25</sup>. The hard sphere model was employed as an effective  $S(Q)$  for all  $W_0$  values.

## Results and Discussion

### Aggregation behavior of cationic surfactant reverse micelles in water/supercritical CO<sub>2</sub> mixtures

In a previous study, visual observation and FT-IR spectra measurements for 16.7 mM [C<sub>6</sub>F<sub>13</sub>mim][C<sub>6</sub>F<sub>13</sub>S]/W/CO<sub>2</sub>  $\mu$ Es were conducted.<sup>25</sup> Those results showed formation of transparent single-phases W/CO<sub>2</sub>  $\mu$ E at pressures above  $P_{\text{trans}}$  in **Fig. S2**, and absorbance characteristic of hydrogen bonded water increased with loading water over the  $W_0$  range from 0 to 50 at 45 °C and 350 bar, suggesting a high water-solubilizing power of  $W_0^{\text{max}} = 50$ .<sup>25</sup> Here, to confirm this observation, solubilization of water and the tracer ionic dye (aqueous methyl orange MO 3 mM) by [C<sub>6</sub>F<sub>13</sub>mim][C<sub>6</sub>F<sub>13</sub>S] reverse micelles was examined. The dye solution was loaded into 16.7 mM cationic surfactant/CO<sub>2</sub> mixtures, and the UV-vis adsorption spectra were measured at different  $W_0$  values. Alone, MO does not dissolve in pure CO<sub>2</sub> but it does dissolve in water, and is generally incorporated within the water-rich pockets of single-phase W/CO<sub>2</sub>  $\mu$ Es, dyeing the systems red.<sup>12,13</sup> The surfactant [C<sub>6</sub>F<sub>13</sub>mim][C<sub>6</sub>F<sub>13</sub>S] formed transparent and reddish single-phase CO<sub>2</sub> systems with the MO solution, however, the other cationic surfactants always remained as precipitates, yielding undyed CO<sub>2</sub> phases.

The UV-vis spectra of MO for [C<sub>6</sub>F<sub>13</sub>mim][C<sub>6</sub>F<sub>13</sub>S] and the other cationic surfactants are displayed in **Figures 2** and **S3** (supporting information), respectively. At 45 °C the spectra showed large and broad absorption peaks of MO, and an absorbance maximum ( $\lambda_{\text{max}}$ ) at ~418 nm independent of  $W_0$ . As  $\lambda_{\text{max}}$  is known to shift to longer wavelengths<sup>12,13</sup> when MO molecules are solubilized in more polar environments, hence  $\lambda_{\text{max}}$  can be employed to gauge microenvironment polarity. Previous experiments with W/CO<sub>2</sub>  $\mu$ Es with anionic hybrid surfactants FC6-HC $n$  and double FC-tail surfactants  $n$ FG(EO)<sub>2</sub> and  $n$ FS(EO)<sub>2</sub> displayed  $\lambda_{\text{max}}$  values at ~420 nm even at different  $W_0$  values and temperatures of 45 and 75 °C,<sup>12,13</sup> consistent with free MO molecules solubilized in the aqueous cores. The similar  $\lambda_{\text{max}}$  values for anionic and cationic surfactants imply that the microenvironmental polarity surrounding MO molecules was essentially unaffected by the different kinds of headgroups, most likely as a result of weak interactions between headgroups and MO molecules.

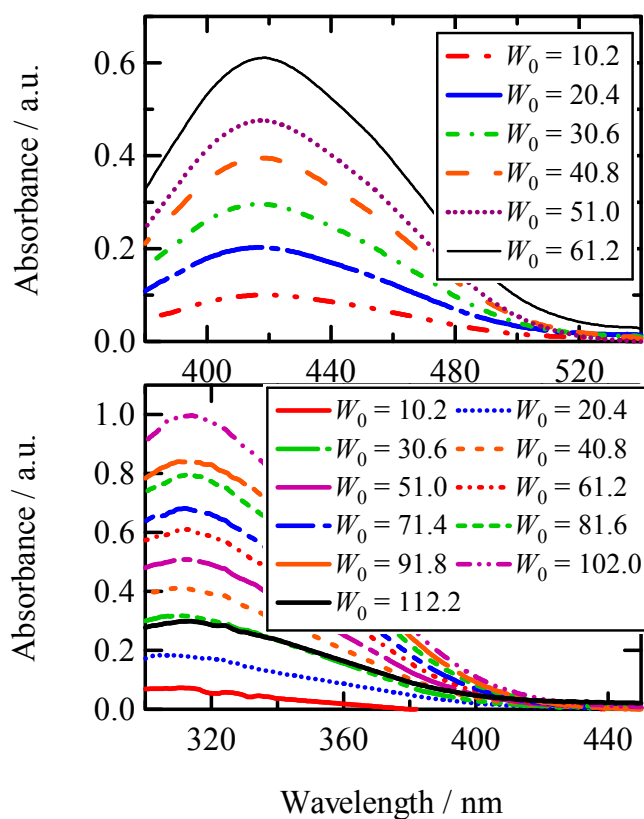


**Figure 2** UV-vis spectra of 16.7mM  $[\text{C}_6\text{F}_{13}\text{mim}][\text{C}_6\text{F}_{13}\text{S}]/\text{water}/\text{CO}_2$  mixtures with different  $W_0$  values at 350 bar and 45 °C (Top) or 75 °C (bottom). 3 mM methyl orange aqueous solution was loaded as a dispersed aqueous phase.

Interestingly, the  $\lambda_{\text{max}}$  values blue-shifted to  $\sim 314$  nm elevating temperature from 45 °C to 75 °C, suggesting a notable change in microenvironment. Such blue shifts with MO have been reported in studies in MO/cationic surfactant/water mixtures, explained by generation of ion pair complexes of MO and cationic surfactants.<sup>34</sup> This suggests that at the high temperature cation-anion dissociation of the cationic surfactant promoted and then formed anionic MO-cationic  $[\text{C}_6\text{F}_{13}\text{mim}]$  ion pair complexes.

As shown in **Figure 2**, the adsorption peaks grew on increasing the dosing of MO solution and the systems remained transparent. To determine the maximum water solubilization ( $W_0^{\text{max}}$ ) of the surfactant at each temperature, the maximum absorbance was plotted as a function of  $W_0$  as shown in **Figure S4**.

1 The linear behavior seen over the  $W_0$  ranges of 0-61.2 at 45 °C and of 0-102 at 75 °C is consistent with  
2  $W_0^{\max}$  values to be ~60 and ~100, respectively. The  $W_0^{\max}$  value at 45 °C was in line with results from FT-  
3 IR spectroscopy in a previous study ( $W_0^{\max} = \sim 50$ )<sup>25</sup>. Such a high value for  $W_0^{\max}$  over 50 is quite rare and  
4 can be identified with a highly efficient surfactant for stabilizing W/CO<sub>2</sub> microemulsions. On the other  
5 hand, no MO absorption was observed for the cationic surfactants [C<sub>6</sub>F<sub>13</sub>mim][(CF<sub>3</sub>)<sub>3</sub>S] and  
6 [C<sub>5</sub>F<sub>11</sub>mim][C<sub>5</sub>F<sub>11</sub>S] (**Figure S3**), suggesting that droplet W/CO<sub>2</sub> μEs, do not form. Since the constituent  
7 surfactants of these cationic surfactants are insoluble and unable to stabilize W/CO<sub>2</sub> μEs,<sup>25</sup> the  
8 synergistic effect of pairing of surfactant anions and cations has been clearly demonstrated by the  
9 formation of [C<sub>6</sub>F<sub>13</sub>mim][C<sub>6</sub>F<sub>13</sub>S]/W/CO<sub>2</sub> microemulsions, which have notably enhanced stability at 75  
10 °C.  
11  
12  
13  
14  
15  
16  
17  
18  
19  
20  
21  
22

23 An important question remaining from the previous study <sup>25</sup> is “why does only  
24 [C<sub>6</sub>F<sub>13</sub>mim][C<sub>6</sub>F<sub>13</sub>S] stabilize W/CO<sub>2</sub> μEs, whereas the other surfactants do not?”. The structural  
25 differences between [C<sub>6</sub>F<sub>13</sub>mim][(CF<sub>3</sub>)<sub>3</sub>S], [C<sub>6</sub>F<sub>13</sub>mim][C<sub>6</sub>F<sub>13</sub>S] and [C<sub>5</sub>F<sub>11</sub>mim][C<sub>5</sub>F<sub>11</sub>S] are small, with  
26 just two more CF<sub>2</sub> units for [C<sub>6</sub>F<sub>13</sub>mim][C<sub>6</sub>F<sub>13</sub>S] than the others. Based on previous studies<sup>7,12,13,32</sup> the  
27 longer double FC-tails in [C<sub>6</sub>F<sub>13</sub>mim][C<sub>6</sub>F<sub>13</sub>S] would be expected to lead to higher CO<sub>2</sub>-philicity and a  
28 greater solubility in scCO<sub>2</sub>. It seems that the total fluorination is important, and for this class of surfactants  
29 there is a critical number of 12 fluorinated carbons needed for stabilization of microemulsions. In other  
30 words, surfactants must (1) be sufficiently compatible (soluble) in scCO<sub>2</sub> to adsorb strongly at the water-  
31 CO<sub>2</sub> interface and (2) have sufficiently thick FC-shells to maintain droplet stability. These phase behavior  
32 studies indicate that [C<sub>6</sub>F<sub>13</sub>mim][C<sub>6</sub>F<sub>13</sub>S] is an optimized surfactant for stabilizing W/CO<sub>2</sub> μEs with high  
33 water loadings over  $W_0^{\max} > 50$ . Furthermore, despite the different cationic structure, this twin-tailed  
34 surfactant is comparable to other super-efficient CO<sub>2</sub>-philic surfactants 8FG(EO)<sub>2</sub> and FC6-HC4 which  
35 instead bear two tails covalently bound to the anionic headgroup <sup>7,12,13,32</sup>.  
36  
37  
38  
39  
40  
41  
42  
43  
44  
45  
46  
47  
48  
49  
50  
51  
52  
53  
54  
55  
56  
57  
58  
59  
60

## Nano-structure of the catanionic surfactant/W/CO<sub>2</sub> microemulsions

1  
2  
3 A previous study of [C<sub>6</sub>F<sub>13</sub>mim][C<sub>6</sub>F<sub>13</sub>S]/W/CO<sub>2</sub> μEs with  $W_0 = 10$  at 350 bar and 45 °C<sup>25</sup>, the  
4  
5 SANS profiles were showed the HP-SANS profiles to be consistent with an ellipsoidal form factor model.  
6  
7 To clarify changes in the core nanostructure with  $W_0$  and pressure, SANS  $I(Q)$  profiles were measured at  
8  
9 45 °C,  $W_0 = 5-35$  and  $P = 120-350$  bar. SANS data along with the fitted  $I(Q)$  functions are shown in **Figure**  
10  
11 **3** (or **Figure S5**). The SANS profiles of [C<sub>6</sub>F<sub>13</sub>mim][C<sub>6</sub>F<sub>13</sub>S]/D<sub>2</sub>O/CO<sub>2</sub> mixtures with  $W_0 \leq 20-25$  at 200-  
12  
13 350 bar and  $\leq 10$  at 120 bar show a gradient of  $\sim 0$  for the  $\log [I(Q)] - \log Q$  plot at  $Q < 0.03 \text{ \AA}^{-1}$ , suggesting  
14  
15 formation of globular nanosized D<sub>2</sub>O cores. All SANS data were always measured under stirring. On the  
16  
17 other hand, when  $W_0$  was  $\geq 25$  at 200-350 bar the scattering intensity increased with decreasing  $Q$  at  $Q <$   
18  
19  $0.02 \text{ \AA}^{-1}$  displaying gradients of  $\sim Q^{-4}$ . At high  $W_0$  values  $\geq 25$  separated water probably remained in the  
20  
21 systems, and was dispersed as equilibrium W/CO<sub>2</sub> emulsion droplets owing to the stirring W/CO<sub>2</sub> μEs.  
22  
23 The SANS also showed gradients of  $\sim Q^{-4}$  at  $Q < 0.02 \text{ \AA}^{-1}$ .  
24  
25  
26  
27

28 As a first step in SANS data analysis, Guinier<sup>33</sup> and Porod<sup>35</sup> plots were used to estimate the D<sub>2</sub>O  
29  
30 core radii (**Figures S6 and S7**), and the results are listed in **Table S1**. The Porod plot asymptote at high  
31  
32  $Q$  can be used to analyze interfacial area per surfactant molecule<sup>35</sup>. Unfortunately, reliable asymptotic  
33  
34  $\{I(Q) Q^4\}_{Q \rightarrow \infty}$  values could not be obtained due to a combination of weak scattering and background noise  
35  
36 as shown in **Figure S7**. SANS data were also analyzed with Ornstein-Zernicke formalism to investigate  
37  
38 density fluctuations in a system approaching critical demixing or phase separation.<sup>36-38</sup> The correlation  
39  
40 lengths  $\zeta$ , showing sizes characteristic of such structural domains are plotted as a function of  $W_0$  in **Figure**  
41  
42 **S9**. The  $\zeta$  values were found to increase from  $\sim 12 \text{ \AA}$  to  $\sim 30 \text{ \AA}$  with increasing  $W_0$  from 10 to 35 and the  
43  
44 increasing trends of  $\zeta$  were similar to those radii obtained from Porod ( $R_{p-sph}$ ) and form fitting analysis  
45  
46 (**Figure 4**). The  $R_{g-sph}$  values from Guinier analysis were employed as initial radii in the subsequent fitting  
47  
48 using models for polydisperse Schultz spherical or ellipsoidal particles, as appropriate for giving the best  
49  
50 fits. In the case of ellipsoids, both oblate and prolate aspect ratios were compared (**Figure S5**), and the  
51  
52 prolate model gave better fits.  
53  
54  
55  
56  
57  
58  
59  
60

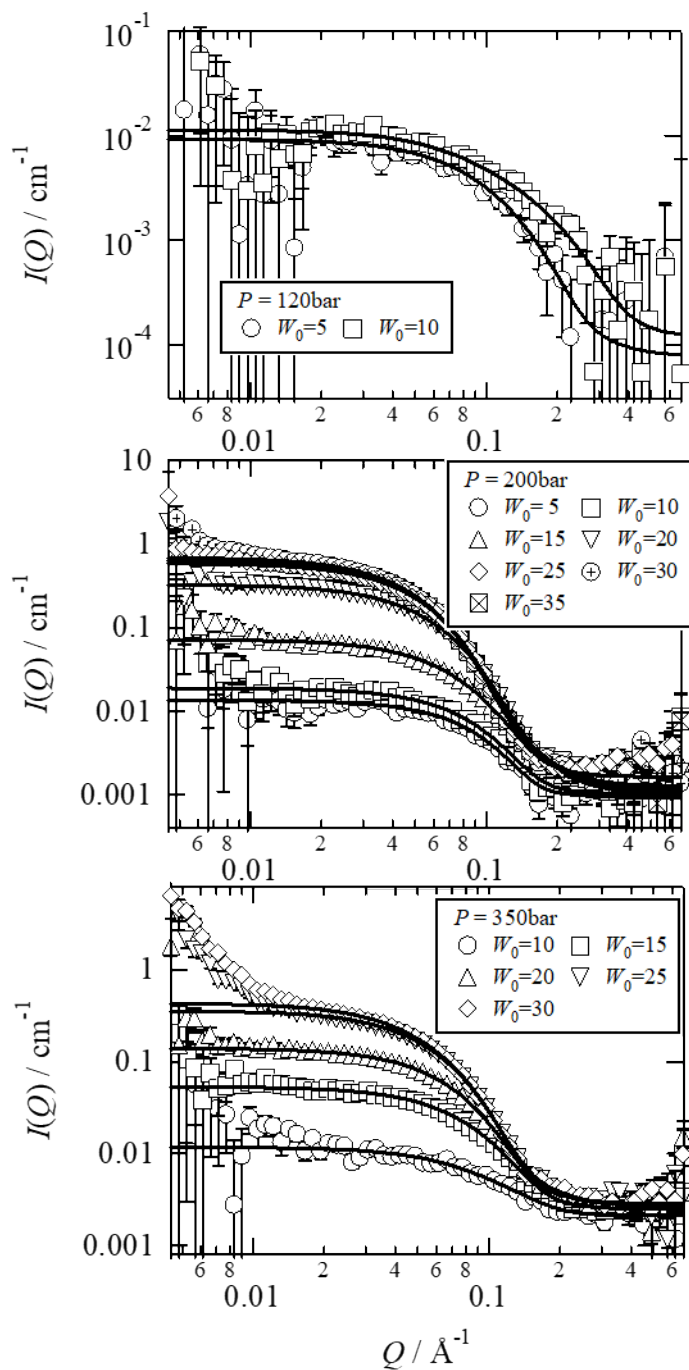


**Figure 3.** SANS profiles of  $D_2O/CO_2$   $\mu E$  with 16.7 mM  $[C_6F_{13}mim][C_6F_{13}S]$  with different  $W_0$  values at 45 °C and 120-350 bar. Solid lines are theoretical curves of prolate ellipsoid particle model fitted to the experimental data.

The model fit parameters for the prolate D<sub>2</sub>O core  $\mu$ E droplets ( $R_{f-ell,a}$  and  $R_{f-ell,b}$ ) are listed in **Table S3**.

To demonstrate droplet growth with increased loading water, equatorial ( $R_{ell-a}$ ) and polar ( $R_{ell-b}$ ) radii of prolate D<sub>2</sub>O cores are plotted in **Figure 4** as a function of  $W_0$  at pressures  $\geq 200$  bar.

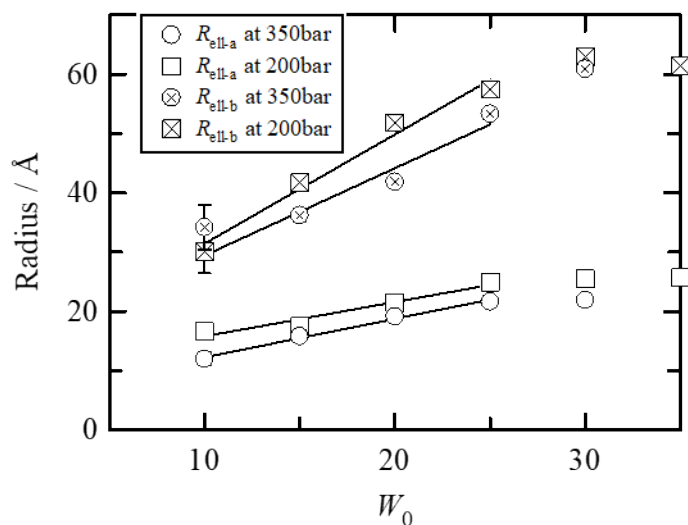


**Figure 4.** Change in prolate ellipsoid radii ( $R_{ell-a}$  and  $R_{ell-b}$ ) for 16.7 mM [C<sub>6</sub>F<sub>13</sub>mim][C<sub>6</sub>F<sub>13</sub>S]/D<sub>2</sub>O/CO<sub>2</sub>  $\mu$ E cores as a function of  $W_0$  at 45 °C and 200 bar or 350 bar.

As seen in **Table S3** at 120 bar the radii reduced with increasing  $W_0$  from 5 to 10, which was accompanied by a phase transition from transparent  $\mu$ Es to turbid phases (i.e. Winsor IV  $\rightarrow$  stirred Winsor II W/CO<sub>2</sub> microemulsions). On the other hand, at pressures  $\geq 200$  bar, the oblate radii increased linearly with  $W_0$  as up to  $W_0 = 25$ , being described by  $(R_{ell-a} / \text{Å}) = a_{ell-a} + b_{ell-a} W_0$  and  $(R_{ell-b} / \text{Å}) = a_{ell-b} + b_{ell-b} W_0$  (where  $a_{ell-a}$ ,  $b_{ell-a}$ ,  $a_{ell-b}$ ,  $b_{ell-b} = 10.0, 0.58, 13.0, 1.84$  at 200 bar, and  $5.79, 0.65, 14.7, 1.47$  at 350 bar. Eventually, the radii reached  $R_{ell-a} = \sim 26$  Å and  $R_{ell-b} = \sim 63$  Å at 200 bar, and  $R_{ell-a} = \sim 22$  Å and  $R_{ell-b} = \sim 61$  Å at 350 bar. This is consistent with swelling behavior with loading water as commonly reported in W/O and W/CO<sub>2</sub> reverse microemulsions<sup>13,32,39</sup>. The radii values seemed to plateau for  $W_0 > 30$  and visually these systems were turbid, consistent with stirred separating Winsor II phases. The slight discrepancies with  $W_0^{\max}$  obtained by spectroscopically may be due to weak stirring power in the pressure



cell and/or use of D<sub>2</sub>O instead of H<sub>2</sub>O needed for the HP-SANS experiments. In contrast with the increasing trend of radii with  $W_0$ , the aspect ratios ( $R_{\text{ell-b}}/R_{\text{ell-a}}$ ) were very similar (1.8-2.9) and seemed to be independent of pressure and  $W_0$  as shown in **Figure S10**. The formation of elongated reverse micelles is an interesting observation, and is expected to increase CO<sub>2</sub> viscosity, which may find applications in CO<sub>2</sub>-EOR efficiency<sup>13,40,41</sup>. Using equations (S4) and (S5) in supporting information (Sec S9), apparent intrinsic and specific viscosities,  $[\eta]$  and  $\eta_{\text{sp}}$ , were estimated (**Table S3**). The viscosity enhancements predicted this way would only be modest, ~13 % or less compared with that of pure CO<sub>2</sub>. Hence, higher surfactant concentration could be needed to promote higher CO<sub>2</sub> thickening.

Previous SANS studies of double FC-tail surfactants  $n\text{FG}(\text{EO})_2$  with different FC lengths ( $n = 4-8$ ) also found a linear relationship between spherical D<sub>2</sub>O core radius,  $R_c$ , and  $W_0$  where  $R_c = a + b W_0$ , and the constants  $a = 5.0-5.4$  and  $b = 0.60-0.64$ <sup>32</sup>. The average values  $a$  and  $b$  of prolate core radii for [C<sub>6</sub>F<sub>13</sub>mim][C<sub>6</sub>F<sub>13</sub>S]/D<sub>2</sub>O/CO<sub>2</sub> microemulsions, namely  $a = (2a_{\text{ell-a}} + a_{\text{ell-b}})/3$  and  $b = (2b_{\text{ell-a}} + b_{\text{ell-b}})/3$ , were 11.0 and 1.00 at 200 bar and 8.8 and 0.92 at 350 bar, and these are 1.7-2.1 and 1.5-1.6 times larger than those for  $n\text{FG}(\text{EO})_2$ , respectively. For spherical geometry the volume of surfactant headgroup ( $v_{\text{head}}$ ) and area per surfactant molecule ( $A$ ), respectively are related by equation (1)

$$\alpha(p) R_c = (3v_{\text{head}}/A) + (3v_w/A) W_0 \quad (1)$$

where  $\alpha(p) = 1 + 2p^2$ ,  $p$  is polydispersity index ( $\sigma/R_c$ ),  $R_c$  is the core radius, and  $v_w$  is volume of a water molecule<sup>13,32</sup>. It follows that the larger  $a$  and  $b$  values suggests [C<sub>6</sub>F<sub>13</sub>mim][C<sub>6</sub>F<sub>13</sub>S] to have a larger  $v_{\text{head}}$  and a smaller  $A$  than for the  $n\text{FG}(\text{EO})_2$  series. Based on Equation (1), a volume-to-surface area ratio per aqueous core in reverse  $\mu\text{E}$  ( $v_{\text{core}}/s_{\text{core}}$ ) can be expressed as,

$$\alpha(p) (v_{\text{core}}/s_{\text{core}}) = (v_{\text{head}} N_{\text{agg}} + v_w W_0 N_{\text{agg}}) / (A N_{\text{agg}}) = (v_{\text{head}}/A) + (v_w/A) W_0 \quad (2)$$

where  $N_{\text{agg}}$  is aggregation number.<sup>13,32</sup> An advantage of using Equation (2) is that it can be applied to a wide range of morphologies (spheres, ellipsoids, rods etc), whereas Equation (1) relates only to spherical morphology. Using equation 2 and assuming constant  $v_{\text{head}}$  and  $A$  for [C<sub>6</sub>F<sub>13</sub>mim][C<sub>6</sub>F<sub>13</sub>S], ( $v_{\text{core}}/s_{\text{core}}$ ) values calculated from  $R_{\text{ell-a}}$  and  $R_{\text{ell-b}}$  were plotted as a function of  $W_0$ , as displayed in **Figure 5**.

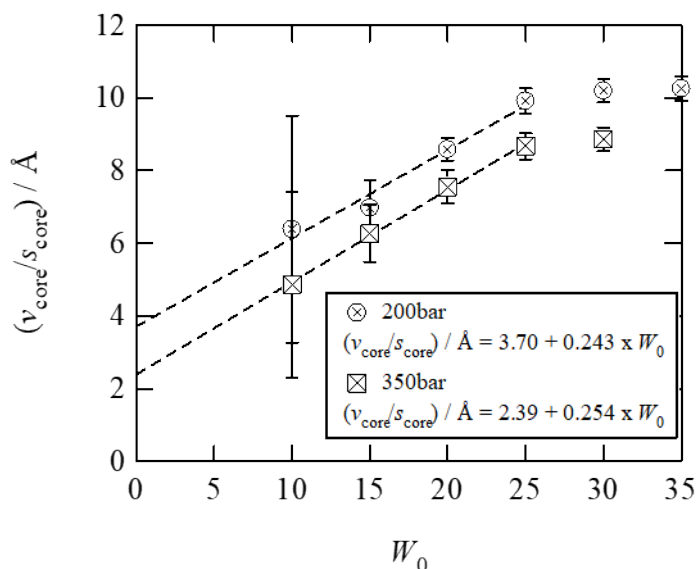


**Figure 5.** Change in  $(v_{\text{core}}/s_{\text{core}})$  of prolate cores in 16.7mM  $[\text{C}_6\text{F}_{13}\text{mim}][\text{C}_6\text{F}_{13}\text{S}]/\text{D}_2\text{O}/\text{CO}_2$   $\mu\text{Es}$  as a function of  $W_0$  at 45 °C and 200 bar or 350 bar.

The  $(v_{\text{core}}/s_{\text{core}})$  data at  $W_0 \leq 25$  were expressed as linear functions, suggesting  $v_{\text{head}}$  and  $A$  can be calculated using Equation (2). The values of  $A$ ,  $v_{\text{head}}$ , and radius of headgroup ( $R_{\text{head}} = (3v_{\text{head}} / 4\pi)^{1/3}$ ) obtained from the slopes and the intercepts were  $(A, v_{\text{head}}, R_{\text{head}}) = (105 \text{ \AA}^2, 459 \text{ \AA}^3, 4.8 \text{ \AA})$  at 200 bar and  $(101 \text{ \AA}^2, 284 \text{ \AA}^3, 4.1 \text{ \AA})$  at 350 bar. At the higher pressures, the headgroup area and volume became smaller, implying a decrease in surfactant cation-anion pair dissociation and/or a decrease in the portion of the head groups immersed in the aqueous cores owing to increased solvation of surfactant tails by  $\text{CO}_2$  at the higher pressure (density). Therefore, the increased  $\text{CO}_2$  pressure (or density) affects not only tail- $\text{CO}_2$  solvation but also interactions between anionic and cationic headgroups. This could lead to a larger EPP and a lower HCB resulting to the smaller  $R_{\text{ell-a}}$  and  $R_{\text{ell-b}}$  (i.e. a larger curvature for smaller droplets) at the higher pressures. As compared with anionic double FC-tail surfactants having a sulfonate group, the  $A$  and  $v_{\text{head}}$  values of  $[\text{C}_6\text{F}_{13}\text{mim}][\text{C}_6\text{F}_{13}\text{S}]$  at 350 bar are similar to the  $n\text{FG}(\text{EO})_2$  and  $n\text{FS}(\text{EO})_2$  (e.g.  $A$  and  $v_{\text{head}}$  were 117-129  $\text{\AA}^2$  and 199-231  $\text{\AA}^3$  for the fluorinated surfactants in  $W/\text{CO}_2$   $\mu\text{Es}$  at 45 °C and 350 bar, respectively). This is interesting, because of the very different head group structures comparing

these two classes of surfactants. The implication is that the high water solubilization capacities of  $[C_6F_{13}mim][C_6F_{13}S]$  in  $W/CO_2$   $\mu$ Es are linked to the electrostatic ion-pairing, promoting larger EPP and lower HCB values comparable to those of the super-efficient double FC-tail surfactants<sup>7,12,32</sup>.

For these  $[C_6F_{13}mim][C_6F_{13}S]$  surfactants in  $scCO_2$ , the reverse micelle aggregation number ( $N_{agg}$ ) and occupied area per surfactant molecule at the  $W/CO_2$  microemulsion interface ( $A_{C/W}$ ) were calculated using the following equations.

$$N_{agg} = C_{surf}/C_{micelle} \quad (3)$$

$$C_{micelle} = (V_{D_2O} C_{D_2O} + V_{head} C_{surf}) / (V_{core}) = C_{surf} (V_{D_2O} W_0 + v_{head} N_A) / (v_{core} N_A) \quad (4)$$

$$A_{C/W} = s_{core}/N_{agg} \quad (5)$$

where  $N_A$  is Avogadro's number,  $C_{surf}$  and  $C_{D_2O}$ ,  $C_{micelle}$  are molar concentrations of surfactant,  $D_2O$  and reverse micelle,  $v_{core}$  is volume per  $D_2O$  core,  $V_{D_2O}$ ,  $V_{head}$ , and  $V_{core}$  are molar volumes of  $D_2O$ , surfactant headgroups and  $D_2O$  cores plus headgroups ( $V_{head} = v_{head} N_A$ ,  $V_{core} = v_{core} N_A$ ), respectively. For the calculation of  $A_{C/W}$  calculation,  $s_{core}$  is surface area per  $D_2O$  core, being calculated using the ellipsoid radii ( $R_{f-ell,a}$  and  $R_{f-ell,b}$ ) as well as the calculation of  $v_{core}$  for  $C_{micelle}$ .

According to theory<sup>26-29</sup> the spontaneous packing parameter (SPP) can be obtained by

$$SPP = v_{tail}/(A_0 l_{tail}) \quad (6)$$

where  $v_{tail}$  and  $l_{tail}$  are hydrophobic tail volume and length, respectively. These symbols have the same meanings as in the expression of the EPP.<sup>29</sup> Entropy is taken into account by the fact that the area per molecule minimizes the free energy of the surfactant film ( $A_0$  is the area that minimizes the free energy). According to this approach reverse micelles would be obtained with  $SPP > 1$  (reversed cores form if the surfactant tails orient upward) to  $\sim 1$  (cylindrical). In the case of  $W/CO_2$   $\mu$ Es, EPP values should be calculated by taking account of solvation of the head and tail groups with water and  $CO_2$  into the  $A_0$  and  $v_{tail}$  values. If the hydrophobic part is assumed to be a truncated cone, the volume should be<sup>13,32</sup>

$$v_{tail} = l_{tail} \{A_{C/W} + A_{tail} + (A_{C/W} A_{tail})^{0.5}\} / 3 \quad (7)$$

where  $A_{tail}$  is area per hydrophobic tail terminus, respectively. When  $A_0$  is replaced by  $A_{C/W}$  for the calculation of EPP in  $W/CO_2$   $\mu$ Es, Eq. (6) can be simply expressed as

$$\text{EPP} = \{s_{\text{micelle}} + s_{\text{core}} + (s_{\text{micelle}} s_{\text{core}})^{0.5}\} / (3s_{\text{core}}) \quad (8)$$

where  $s_{\text{micelle}}$  is surface area per reverse micelle. In this study, the values of  $s_{\text{micelle}}$  were calculated from the ellipsoid core radii ( $R_{\text{f-ell,a}}$  and  $R_{\text{f-ell,b}}$ ), with surfactant tail length  $l_{\text{tail}}$  assumed to be 13.6 Å (between the terminal F-atom and the C-atom bearing the sulfonate group). All the values of  $A_{C/W}$ ,  $N_{\text{agg}}$  and EPP obtained by Eqs. (3)-(8) are based on the assumption that all surfactant molecules are adsorbed at the W/CO<sub>2</sub> interface. In actual W/CO<sub>2</sub> μEs, it is likely that some surfactant molecules will partition away from the interface. However, this is estimated to be negligible compared with total number of associated surfactant molecules ( $8.0 \times 10^{-2}$  mol%), taking into account very low critical microemulsion concentrations in scCO<sub>2</sub> for fluorinated ionic surfactants, which is typically  $< 10^{-4}$  mol %.<sup>42</sup> The calculated aggregation properties  $N_{\text{agg}}$ ,  $A_{C/W}$ , and EPP for the prolate droplets are listed in **Table S4**. The  $A_{C/W}$  values were 118-134 Å<sup>2</sup> at  $W_0$  values of 10-30 and are very close to those of  $n\text{FG}(\text{EO})_2$  and  $n\text{FS}(\text{EO})_2$  as mentioned above.<sup>32</sup>

**Figure 6** shows changes in  $N_{\text{agg}}$  and EPP as a function of  $W_0$  for  $[\text{C}_6\text{F}_{13}\text{mim}][\text{C}_6\text{F}_{13}\text{S}]/\text{D}_2\text{O}/\text{CO}_2$  microemulsions at 45 °C and 200 and 350 bar, using data from **Table S4**. For comparison purposes, the figures also include literature data for double-tail surfactants  $n\text{FG}(\text{EO})_2$  ( $n = 4$  and 8) in W/CO<sub>2</sub> μEs<sup>32</sup> and the common hydrocarbon surfactant AOT but in W/*n*-heptane μEs<sup>43</sup>.

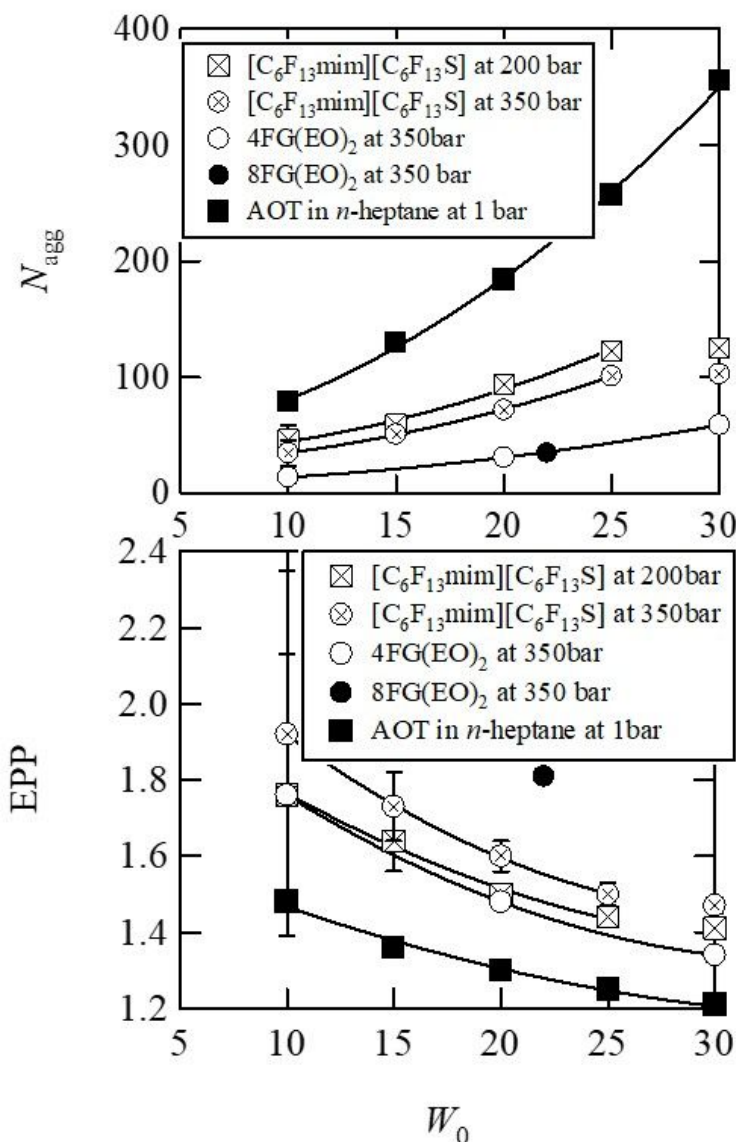


**Figure 6.** Changes in aggregation number ( $N_{agg}$ ) and effective packing parameter (EPP) of surfactants as a function of  $W_0$ . The data were for D<sub>2</sub>O/CO<sub>2</sub>  $\mu$ Es containing 16.7 mM [C<sub>6</sub>F<sub>13</sub>mim][C<sub>6</sub>F<sub>13</sub>S] and 50 mM double FC-tail surfactants (4FG(EO)<sub>2</sub> and 8FG(EO)<sub>2</sub>) at 45 °C and W/*n*-heptane  $\mu$ Es containing 50 mM AOT at 25 °C.

As reported for other reverse micellar systems with AOT<sup>43</sup> and the double FC-tail surfactants<sup>32</sup>,  $N_{\text{agg}}$  and EPP for [C<sub>6</sub>F<sub>13</sub>mim][C<sub>6</sub>F<sub>13</sub>S], respectively, increased and decreased with  $W_0$ , until the single phase  $\mu\text{Es}$  became unstable and turbid phases appeared. This is consistent with an increase in aggregation number for both surfactant and water, as well as a change in surfactant molecular morphology from a reversed truncated cone to a cylindrical shape. These changes are linked to growth of reverse micelles and a decrease in negative curvature of the W/CO<sub>2</sub> interface with increasing water loading. As compared to the double FC-tail anionic 8FG(EO)<sub>2</sub> and 4FG(EO)<sub>2</sub> surfactants, the catanionic [C<sub>6</sub>F<sub>13</sub>mim][C<sub>6</sub>F<sub>13</sub>S] generates reverse micelles with larger  $N_{\text{agg}}$  values than those anionics. This implies that headgroup ion-pairing promotes dense packing of [C<sub>6</sub>F<sub>13</sub>mim][C<sub>6</sub>F<sub>13</sub>S] molecules to favor reverse micelles owing to reduced electrostatic repulsion between headgroups. On the other hand, lowering the pressure from 350 to 200 bar increased  $N_{\text{agg}}$  and decreased EPP for [C<sub>6</sub>F<sub>13</sub>mim][C<sub>6</sub>F<sub>13</sub>S], presumably due to a promotion of molecular aggregation owing to a reduction in CO<sub>2</sub> solvation of the fluorinated tails at the lower CO<sub>2</sub> density. Comparing the  $A_{C/W}$  and  $v_{\text{head}}$  values for [C<sub>6</sub>F<sub>13</sub>mim][C<sub>6</sub>F<sub>13</sub>S] and the fluorinated double-tail 8FG(EO)<sub>2</sub> and 4FG(EO)<sub>2</sub>, shows EPP was relatively close to that of 4FG(EO)<sub>2</sub> but far from the value for 8FG(EO)<sub>2</sub>. Since these two surfactant classes have similar  $A_{C/W}$  values, the difference in EPP between them is likely due to the fluorination level of the tails, namely longer FC-tails have the capacity to solvate more CO<sub>2</sub> molecules, giving rise to greater effective tail volumes. As compared with AOT/W/*n*-heptane  $\mu\text{Es}$ <sup>43</sup>, the W/CO<sub>2</sub>  $\mu\text{Es}$  had smaller  $N_{\text{agg}}$  and larger EPP values. This may be linked to differences in surfactant tail-solvent interactions, in other words, better solvation for the FC-tails with CO<sub>2</sub>, as compared to for the AOT-tails with *n*-heptane.

This study demonstrated that the EPP of this catanionic surfactant, comparable to that of anionic double FC-tail surfactants, enables stabilization of W/CO<sub>2</sub> microemulsions with high  $W_0$  values. This is very interesting as ionic headgroups themselves are known to be insoluble in supercritical CO<sub>2</sub> and surfactants having ionic head groups usually require long and/or multiple CO<sub>2</sub>-philic tails to stabilize W/CO<sub>2</sub> microemulsions. However, it is now apparent that mixing single CO<sub>2</sub>-philic tail anions and cations,

1 which are alone mostly insoluble and incompatible with CO<sub>2</sub>, is a useful approach to design CO<sub>2</sub>-philic  
2 surfactants.  
3  
4  
5  
6  
7  
8  
9  
10  
11  
12  
13  
14  
15  
16  
17  
18  
19  
20  
21  
22  
23  
24  
25  
26  
27  
28  
29  
30  
31  
32  
33  
34  
35  
36  
37  
38  
39  
40  
41  
42  
43  
44  
45  
46  
47  
48  
49  
50  
51  
52  
53  
54  
55  
56  
57  
58  
59  
60

## Conclusions

In order to meet requirements for potential use of W/CO<sub>2</sub> μEs in industrial processes<sup>16-18</sup>, W/CO<sub>2</sub> μEs have been studied here, stabilized by ion-pairs of low F-content surfactant anions and cations, which themselves are individually insoluble and surface-inactive in scCO<sub>2</sub>. Because the ions are strongly associated, they cannot be easily dissociated under ambient conditions, as such, catanionic surfactants are not classified as normal ionic surfactants<sup>25,44,45</sup>.

This study was conceived to answer the question “why are ion-paired catanionic surfactants so effective at stabilizing high water content W/CO<sub>2</sub> μEs”? The three new significant findings are:-

- (1) The W/CO<sub>2</sub> μEs with [C<sub>6</sub>F<sub>13</sub>mim][C<sub>6</sub>F<sub>13</sub>S] solubilized an ionic dye which acts as a microenvironmental polarity probe, showing behavior similarity to other fluorinated anionic surfactants.<sup>9,12</sup> On the other hand, the other catanionic surfactants with lower F-content did not solubilize the dye in scCO<sub>2</sub>, which is consistent with a lack of W/CO<sub>2</sub> μE stabilization.
- (2) Aggregation numbers of reverse micelles were about two times larger for [C<sub>6</sub>F<sub>13</sub>mim][C<sub>6</sub>F<sub>13</sub>S] compared with fluorinated double-tail anionic surfactants<sup>32</sup> implying that electrostatic interactions between cationic and anionic headgroups promote close packing of surfactants to stabilize reverse micelles.
- (3) Effective packing parameter (EPP) values of the catanionic surfactant in W/CO<sub>2</sub> μEs were relatively close to those found previously for the double perfluorooctyl-tail anionic surfactant 4FG(EO)<sub>2</sub><sup>32</sup>. This indicates the electrostatic interactions resulted in a small interfacial areas and volumes for the catanionic headgroups, which is required for reversed curvature self-assembly, as found for the sulfonate headgroup of 4FG(EO)<sub>2</sub><sup>32</sup>.

From these findings and previous studies<sup>25</sup>, the efficiency of [C<sub>6</sub>F<sub>13</sub>mim][C<sub>6</sub>F<sub>13</sub>S] is likely related to EPP and HCB would be consistent with those of double FC-tail anionic surfactants<sup>32</sup>. Such a large EPP and a low HCB would be consistent with the small area and low ionicity of the catanionic headgroup, as compared to the related single-tail and single ionic headgroup anionic and cationic surfactants



1 (Na[C<sub>6</sub>F<sub>13</sub>S] and [C<sub>6</sub>F<sub>13</sub>mim][CH<sub>3</sub>SO<sub>3</sub>]). Hence, the concept of surfactant anion-cation pairing represents  
2 a new platform for developing CO<sub>2</sub>-philic surfactants and water-in-CO<sub>2</sub> microemulsions for practical  
3 applications. This surfactant may be thought of as “the goose (cheap, simple-structure, and CO<sub>2</sub>-inactive  
4 surfactants) that lays the golden egg (super-efficient CO<sub>2</sub>-philic solubilizer)”. Using this platform but with  
5 highly-methylated alkyl tails, it should be possible to generate cheap and simple hydrocarbon surfactants  
6 as a super-efficient CO<sub>2</sub>-philic solubilizers, which is a long-cherished dream in supercritical CO<sub>2</sub> science  
7 and technology.  
8  
9  
10  
11  
12  
13  
14  
15  
16  
17  
18  
19  
20  
21  
22  
23  
24  
25  
26  
27  
28  
29  
30  
31  
32  
33  
34  
35  
36  
37  
38  
39  
40  
41  
42  
43  
44  
45  
46  
47  
48  
49  
50  
51  
52  
53  
54  
55  
56  
57  
58  
59  
60

## ASSOCIATED CONTENT

**Supporting Information.** Chemical structures of surfactants studied in earlier W/CO<sub>2</sub> microemulsion studies. Calculation of scattering length densities of reverse micelle shells ( $\rho_{\text{shell}}$ ), aqueous cores ( $\rho_{\text{core}}$ ), and CO<sub>2</sub> ( $\rho_{\text{CO}_2}$ ) in the D<sub>2</sub>O/CO<sub>2</sub>  $\mu$ Es. Pressures at which clear single phases start to appear cloudy,  $P_{\text{trans}}$  for [C<sub>6</sub>F<sub>13</sub>mim][C<sub>6</sub>F<sub>13</sub>S]/W/CO<sub>2</sub> mixtures. UV-vis absorption spectra for aqueous methyl orange (MO) solution/CO<sub>2</sub> mixtures with 16.7 mM [C<sub>5</sub>F<sub>11</sub>mim][C<sub>5</sub>F<sub>11</sub>S] and [C<sub>6</sub>F<sub>13</sub>mim][(CF<sub>3</sub>)<sub>3</sub>S]. Change in absorbance of [C<sub>6</sub>F<sub>13</sub>mim][C<sub>6</sub>F<sub>13</sub>S]/W/CO<sub>2</sub>  $\mu$ Es with adding aqueous methyl orange (MO) solution. SANS profiles (Lin-Lin plots) for 16.7mM [C<sub>6</sub>F<sub>13</sub>mim][C<sub>6</sub>F<sub>13</sub>S]/D<sub>2</sub>O/CO<sub>2</sub>  $\mu$ Es at various  $W_0$  values and pressures. Estimation of D<sub>2</sub>O core radii in 16.7 mM [C<sub>6</sub>F<sub>13</sub>mim][C<sub>6</sub>F<sub>13</sub>S]/D<sub>2</sub>O/CO<sub>2</sub> reverse micelles by Guinier and Porod analyses of SANS data. Estimation of correlation length for 16.7 mM [C<sub>6</sub>F<sub>13</sub>mim][C<sub>6</sub>F<sub>13</sub>S]/D<sub>2</sub>O/CO<sub>2</sub> microemulsions by Ornstein-Zernicke formalism. Prolate D<sub>2</sub>O core radius, aspect ratio, estimated specific viscosity for 16.7 mM [C<sub>6</sub>F<sub>13</sub>mim][C<sub>6</sub>F<sub>13</sub>S]/D<sub>2</sub>O/CO<sub>2</sub> microemulsions obtained by fitting theoretical curves of prolate ellipsoidal particle model to SANS data. Estimation of reverse micelle concentration, aggregation number, area per surfactant molecule, and effective packing parameter of the D<sub>2</sub>O/CO<sub>2</sub>  $\mu$ Es with 16.7 mM [C<sub>6</sub>F<sub>13</sub>mim][C<sub>6</sub>F<sub>13</sub>S] at 45 °C and 200 bar or 350 bar.

This material is available free of charge via the Internet at “<http://pubs.acs.org>.”

## AUTHOR INFORMATION

**Corresponding Author.** \*E-mail [sagisaka@hirosaki-u.ac.jp](mailto:sagisaka@hirosaki-u.ac.jp); FAX +81-172-39-3579 (M.S.)

Notes. The authors declare no competing financial interest.

## ACKNOWLEDGEMENT

This project was supported by JSPS [KAKENHI, Grant-in-Aid for Scientific Research (B), No. 19H02504, Fostering Joint International Research (A), No. 15KK0221, Grant-in-Aid for Challenging Research (Exploratory), No.17K19002], and Leading Research Organizations (RCUK [through EPSRC EP/I018301/1], ANR [13-G8ME-0003]) under the G8 Research Councils Initiative for Multilateral

1 Research Funding –G8-2012. We also acknowledge STFC for the allocation of beam time, travel, and  
2 consumables grants at ISIS.  
3  
4  
5  
6  
7  
8  
9  
10  
11  
12  
13  
14  
15  
16  
17  
18  
19  
20  
21  
22  
23  
24  
25  
26  
27  
28  
29  
30  
31  
32  
33  
34  
35  
36  
37  
38  
39  
40  
41  
42  
43  
44  
45  
46  
47  
48  
49  
50  
51  
52  
53  
54  
55  
56  
57  
58  
59  
60

## References

- 1  
2  
3  
4 (1) Beckman, E. J. Supercritical and Near-Critical CO<sub>2</sub> in Green Chemical Synthesis and Processing. *J.*  
5  
6 *Supercrit. Fluids* **2004**, *28*, 121-191.  
7  
8  
9 (2) Goetheer, E. L. V.; Vortaman, M. A. G.; Keurentjes, J. T. F. Opportunities for Process Intensification  
10  
11 Using Reverse Micelles in Liquid and Supercritical Carbon Dioxide. *Chem. Eng. Sci.* **1999**, *54*, 1589-  
12  
13 1596.  
14  
15  
16 (3) Consani, K. A.; Smith, R. D. Observations on the Solubility of Surfactants and Related Molecules in  
17  
18 Carbon Dioxide at 50 °C. *J. Supercrit. Fluids* **1990**, *3*, 51-65.  
19  
20  
21 (4) Ryoo, W.; Webber, S. E.; Johnston, K. P. Water-in-Carbon Dioxide Microemulsions with Methylated  
22  
23 Branched Hydrocarbon Surfactants. *Ind. Eng. Chem. Res.*, **2003**, *42*, 6348-6358.  
24  
25  
26  
27 (5) Lee, H.; Pack, J W.; Wang, W.; Thurecht, K. J.; Howdle, S. M. Synthesis and Phase Behavior of CO<sub>2</sub>-  
28  
29 Soluble Hydrocarbon Copolymer: Poly(Vinyl Acetate-*alt*-Dibutyl Maleate). *Macromolecules* **2010**, *43*,  
30  
31 2276-2282.  
32  
33  
34  
35 (6) Shi, Q.; Jing, L.; Xiong, C.; Liu, C.; Qiao, W. Solubility of Nonionic Hydrocarbon Surfactants with  
36  
37 Different Hydrophobic Tails in Supercritical CO<sub>2</sub>. *J. Chem. Eng. Data* **2015**, *60*, 2469–2476.  
38  
39  
40  
41 (7) Sagisaka, M.; Yoda, S.; Takebayashi, Y.; Otake, K.; Kitiyanan, B.; Kondo, Y.; Yoshino, N.;  
42  
43 Takebayashi, K.; Sakai, H.; Abe, M. Preparation of a W/scCO<sub>2</sub> Microemulsion Using Fluorinated  
44  
45 Surfactants. *Langmuir* **2003**, *19*, 220-225.  
46  
47  
48 (8) Lee, C. T., Jr.; Psathas, P. A.; Johnston, K. P.; deGrazia, J.; Randolph, T. W. Water-in-Carbon Dioxide  
49  
50 Emulsions: Formation and Stability. *Langmuir* **1999**, *15*, 6781-6791.  
51  
52  
53  
54  
55  
56  
57  
58  
59  
60

- 1 (9) Johnston, K. P.; Harrison, K. L.; Klarke, M. J.; Howdle, S. M.; Heitz, M. P.; Bright, F. V.; Carlier, C.;  
2 Randolph, T. W. Water-in-Carbon Dioxide Microemulsions: A New Environment for Hydrophiles  
3 Including Proteins. *Science* **1996**, *271*, 624-626.  
4  
5  
6  
7 (10) Zielinski, R. G.; Kline, S. R.; Kaler, E. W.; Rosov, N. A Small-Angle Neutron Scattering Study of  
8 Water in Carbon Dioxide Microemulsions. *Langmuir* **1997**, *13*, 3934-3937.  
9  
10  
11  
12 (11) Niemeyer, E. D.; Bright, F. V. The pH within PFPE Reverse Micelles Formed in Supercritical CO<sub>2</sub>.  
13 *J. Phys. Chem. B* **1998**, *102*, 1474-1478.  
14  
15  
16  
17 (12) Sagisaka, M.; Iwama, S.; Yoshizawa, A.; Mohamed, A.; Cummings S.; Eastoe, J. An Effective and  
18 Efficient Surfactant for CO<sub>2</sub> Having Only Short Fluorocarbon Chains. *Langmuir* **2012**, *28*, 10988-10996.  
19  
20  
21  
22 (13) Sagisaka, M.; Ono, S.; James, C.; Yoshizawa, A.; Mohamed, A.; Guittard, F.; Enick, R. M.; Rogers,  
23 S. E.; Czajka, A.; Hill, C.; Eastoe, J. Anisotropic Reversed Micelles with Fluorocarbon-Hydrocarbon  
24 Hybrid Surfactants in Supercritical CO<sub>2</sub>. *Colloids Surf. B* **2018**, *168*, 201-210.  
25  
26  
27  
28 (14) Li, Q.; Li, T.; Wu, J. Water Solubilization Capacity and Conductance Behaviors of AOT and  
29 NaDEHP Systems in the Presence of Additives. *Colloids Surf. A* **2002**, *197*, 101-109.  
30  
31  
32  
33 (15) Sagisaka, M.; Hino, M.; Sakai, H.; Abe, M.; Yoshizawa, A. Water/Supercritical CO<sub>2</sub> Microemulsions  
34 with a Fluorinated Double-tail Surfactant for Syntheses of Semiconductor Ultrafine Particles. *J. Jpn.*  
35 *Colour Soc. Mater.* **2008**, *81*, 331-340.  
36  
37  
38  
39 (16) Holmes, J. D.; Steytler, D. C.; Rees, G. D.; Robinson B. H. Bioconversions in a Water-in-CO<sub>2</sub>  
40 Microemulsion. *Langmuir* **1998**, *14*, 6371-6376.  
41  
42  
43  
44 (17) Van Roosmalen, M. J. E.; Woerlee, G. F.; Witkamp, G. J.; Surfactants for Particulate Soil Removal  
45 in Dry-cleaning with High-pressure Carbon Dioxide. *J. Supercrit. Fluids* **2004**, *30*, 97-109.  
46  
47  
48  
49  
50  
51  
52  
53  
54  
55  
56  
57  
58  
59  
60

- 1  
2  
3  
4  
5  
6  
7  
8  
9  
10  
11  
12  
13  
14  
15  
16  
17  
18  
19  
20  
21  
22  
23  
24  
25  
26  
27  
28  
29  
30  
31  
32  
33  
34  
35  
36  
37  
38  
39  
40  
41  
42  
43  
44  
45  
46  
47  
48  
49  
50  
51  
52  
53  
54  
55  
56  
57  
58  
59  
60
- (18) Luo, D.; Qiu, T.; Lu, Q. Ultrasound-assisted Extraction of Ginsenosides in Supercritical CO<sub>2</sub> Reverse Microemulsions. *J. Sci. Food Agric.* **2007**, *87*, 431-436.
- (19) Kravetz, L.; Guin, K. F. Effects of Surfactant Structure on Stability of Enzymes Formulated into Laundry Liquids. *J. Am. Oil Chem. Soc.* **1985**, *62*, 943-949.
- (20) Sagisaka, M.; Fujii, T.; Koike, D.; Yoda, S.; Takebayashi, Y.; Furuya, T.; Yoshizawa, A.; Sakai, H.; Abe, M.; Otake, K. Surfactant-Mixing Effects on the Interfacial Tension and the Microemulsion Formation in Water/Supercritical CO<sub>2</sub> System. *Langmuir* **2007**, *23*, 2369-2375.
- (21) Sagisaka, M.; Koike, D.; Mashimo, Y.; Yoda, S.; Takebayashi, Y.; Furuya, T.; Yoshizawa, A.; Sakai, H.; Abe, M.; Otake, K. Water/supercritical CO<sub>2</sub> Microemulsions with Mixed Surfactant Systems. *Langmuir* **2008**, *24*, 10116–10122.
- (22) Huang, J.-B.; Zhao, G. -X. Formation and Coexistence of the Micelles and Vesicles in Mixed Solution of Cationic and Anionic Surfactant. *Colloid Polym. Sci.* **1995**, *273*, 156–164.
- (23) Upadhyaya, A.; Acosta, E. J.; Scamehorn, J. F.; Sabatini, D. A. Microemulsion Phase Behavior of Anionic-Cationic Surfactant Mixtures: Effect of Tail Branching. *J. Surfactants Deterg.* **2006**, *9*, 169-179.
- (24) Eastoe, J.; Dalton, J.; Rogueda, P.; Sharpe, D.; Dong, J.; Webster, J. R. P. Interfacial Properties of a Catanionic Surfactant. *Langmuir* **1996**, *12*, 2706-2711.
- (25) Sagisaka, M.; Saito, T.; Yoshizawa, A.; Rogers, S. E.; Guittard, F.; Hill, C.; Eastoe, J.; Blesic, M. Water-in-CO<sub>2</sub> Microemulsions Stabilized by Fluorinated Cation–Anion Surfactant Pairs. *Langmuir* **2019**, *35*, 3445–3454.
- (26) Pleines, M.; Kunz, W.; Zemb, T. Understanding and Prediction of the Clouding Phenomenon by Spontaneous and Effective Packing Concepts. *J. Surfact. Deterg.* **2019**, *22*, 1011–1021.

- 1 (27) Ontiveros, J. F.; Pierlot, C.; Catté, M.; Molinier, V.; Pizzino, A.; Salager, J.-L.; Aubry, J.-M.  
2 Classification of ester oils according to their Equivalent Alkane Carbon Number (EACN) and asymmetry  
3 of fish diagrams of C<sub>10</sub>E<sub>4</sub>/ester oil/water systems. *J. Colloid Interf. Sci.* **2013**, *403*, 67–76.  
4  
5  
6  
7 (28) Israelachvili, J. N. Measurements of Hydration Forces Between Macroscopic Surfaces. *Chem. Scr.*  
8 **1985**, *25*, 7-14.  
9  
10  
11  
12 (29) Nagarajan, R. Molecular Packing Parameter and Surfactant Self-Assembly: The Neglected Role of  
13 the Surfactant Tail. *Langmuir* **2002**, *18*, 31–38.  
14  
15  
16  
17 (30) Span, R.; Wagner, W. A New Equation of State for Carbon Dioxide Covering the Fluid Region from  
18 the Triple-Point Temperature to 1100 K at Pressures up to 800 MPa. *J. Phys. Chem. Ref. Data* **1996**, *25*,  
19 1509-1596.  
20  
21  
22  
23  
24  
25  
26 (31) Kotlarchyk, M.; Chen, S.-H.; Huang, J. S.; Kim, M. W. Structure of Three-Component.  
27 Microemulsions in the Critical Region Determined by Small Angle Neutron Scattering Data. *Phys. Rev.*  
28 *A* **1984**, *29*, 2054-2069.  
29  
30  
31  
32  
33 (32) Sagisaka, M.; Iwama, S.; Ono, S.; Yoshizawa, A.; Mohamed, A.; Cummings, S.; Yan, C.; James, C.;  
34 Rogers, S. E.; Heenan, R. K.; Eastoe, J. Nanostructures in Water-in-CO<sub>2</sub> Microemulsions Stabilized by  
35 Double-chain Fluorocarbon Solubilizers. *Langmuir* **2013**, *29*, 7618–7628.  
36  
37  
38  
39  
40  
41 (33) Guinier, A.; Fournet, G. *Small-Angle Scattering of X-Rays*, Wiley, New York, 1956.  
42  
43  
44 (34) Karukstis, K. K.; Savin, D. A.; Loftus, C.T.; D'Angelo, N. D. Spectroscopic Studies of the Interaction  
45 of Methyl Orange with Cationic Alkyltrimethylammonium Bromide Surfactants. *J. Colloid Interf. Sci.*  
46 **1998**, *203*, 157–163.  
47  
48  
49  
50  
51 (35) Kline, S. R. Reduction and Analysis of SANS and USANS Data Using IGOR Pro. *J. Appl. Cryst.*  
52 **2006**, *39*, 895–900.  
53  
54  
55  
56  
57  
58  
59  
60

- 1  
2  
3  
4  
5  
6  
7  
8  
9  
10  
11  
12  
13  
14  
15  
16  
17  
18  
19  
20  
21  
22  
23  
24  
25  
26  
27  
28  
29  
30  
31  
32  
33  
34  
35  
36  
37  
38  
39  
40  
41  
42  
43  
44  
45  
46  
47  
48  
49  
50  
51  
52  
53  
54  
55  
56  
57  
58  
59  
60
- (36) Almásy, L.; Turmine, M.; Perera, A. Structure of Aqueous Solutions of Ionic Liquid 1-Butyl-3-methylimidazolium Tetrafluoroborate by Small-Angle Neutron Scattering. *J. Phys. Chem. B* **2008**, *112*, 2382- 2387.
- (37) Zemb, T. N.; Klossek, M.; Lopian, T.; Marcus, J.; Schöetl, S.; Horinek, D.; Prevost, S. F.; Touraud, D.; Diat, O.; Marčelja, S.; Kunz, W. How to Explain Microemulsions Formed by Solvent Mixtures without Conventional Surfactants. *Proc. Natl. Acad. Sci.* **2016**, *113*, 4260–4265.
- (38) Grimaldi, N.; Rojas, P. E.; Stehle, S.; Cordoba, A.; Schweins, R.; Sala, S.; Luelsdorf, S.; Piña, D.; Veciana, J.; Faraudo, J.; Triolo, A.; Braeuer, A. S.; Ventosa, N. Pressure-Responsive, Surfactant-Free CO<sub>2</sub>-Based Nanostructured Fluids. *ACS Nano* **2017**, *11*, 10774–10784.
- (39) Weber, A.; Stühn, B. Structure and Phase Behavior of Polymer Loaded Non-ionic and Anionic Microemulsions. *J. Chem. Phys.* **2016**, *144*, 144903.
- (40) Williams, D. F. Extraction with Supercritical Gases. *Chem. Eng. Sci.* **1981**, *36*, 1769-1788.
- (41) Orr, F. M.; Taber, J. J. Use of Carbon Dioxide in Enhanced Oil Recovery. *Science* **1984**, *224*, 563-569.
- (42) Sagisaka, M.; Fujii, T.; Ozaki, Y.; Yoda, S.; Takebayashi, Y.; Kondo, Y.; Yoshino, N.; Sakai, H.; Abe, M.; Otake, K. Interfacial Properties of Branch-Tailed Fluorinated Surfactants Yielding a Water/Supercritical CO<sub>2</sub> Microemulsion. *Langmuir* **2004**, *20*, 2560-2566.
- (43) Nave, S.; Eastoe, J.; Heenan, R.K.; Steytler, D.; Grillo, I. What is so Special about Aerosol-OT? 2. Microemulsion Systems. *Langmuir* **2000**, *16*, 8741-8748.
- (44) Yin, H.; Lin, Y.; Huang, J.; Ye, J. Temperature-Induced Vesicle Aggregation in Catanionic Surfactant Systems: The Effects of the Headgroup and Counterion. *Langmuir* **2007**, *23*, 4225–4230.



1 (45) Nakama, Y.; Harusawa, F.; Murotani, I. Cloud Point Phenomena in Mixtures of Anionic and Cationic  
2 Surfactants in Aqueous Solution. *J. Surfactants Deterg.* **1990**, *67*, 717-721.  
3  
4  
5  
6  
7  
8  
9  
10  
11  
12  
13  
14  
15  
16  
17  
18  
19  
20  
21  
22  
23  
24  
25  
26  
27  
28  
29  
30  
31  
32  
33  
34  
35  
36  
37  
38  
39  
40  
41  
42  
43  
44  
45  
46  
47  
48  
49  
50  
51  
52  
53  
54  
55  
56  
57  
58  
59  
60

## TOC (Revised)

Sagisaka, M. et al.

